

**ANALYSIS OF THE SEASONAL EFFECTS ON CESIUM CLOCKS
TO IMPROVE THE LONG-TERM STABILITY OF A TIME SCALE**

E. Bava, F. Cordara, V. Pettiti, P. Tavella(*)
Istituto Elettrotecnico Nazionale Galileo Ferraris
C.so Massimo d'Azeglio, 42
10125 Torino, Italy

(*) Associazione Nazionale Galileo Ferraris Grant

ABSTRACT

The Istituto Elettrotecnico Nazionale time scale UTC(IEN) is generated by a commercial cesium clock selected among the five presently at disposal and is maintained in agreement within 5 microseconds with UTC by means of a phase microstepper.

The problem of the influence of the environmental parameters on atomic clocks has been investigated and recent improvements in the international synchronization systems have shown more clearly the presence of seasonal effects on clocks.

On the IEN cesium clock ensemble, long term frequency instabilities and seasonal variations have been detected and a relationship between humidity and frequency variations has been analyzed. This investigation has been also extended to the cesium clocks kept in the (ISPT) Laboratory in Roma.

An evaluation of the annual repetition of these effects has been performed by means of statistical processes to settle a better use of microstepper corrections and optimize the long term stability of UTC(IEN) time scale.

1. Introduction

The influence of environmental conditions on the commercial cesium clock behaviour has been analyzed in the past and reported in the literature [1,2,3,4] where sensitivity to temperature and humidity variations was pointed out.

In spite of the careful investigations already performed, it has not yet been possible to relate clearly the amount of the rate changes of the clocks considered to the variations introduced in their environmental conditions. Moreover, the results we have at disposal [2,5], have demonstrated that each clock must be analyzed separately to find out a "best estimate" of its long term behaviour where sensible changes in its environment can be expected. This is instrumental in maintaining a time scale of a laboratory in close agreement with

the international atomic time scale if the source of the local UTC is a cesium clock, whose rate is periodically adjusted, and/or if it is a paper time scale computed from a clock ensemble.

2. Long term behaviour of the UTC(IEN) time scale

The Istituto Elettrotecnico Nazionale time scale UTC(IEN) is realized by means of five commercial cesium beam standards [6], that are kept at a temperature of $24 \pm 0.5^\circ\text{C}$ in a room located 12 meters underground.

The laboratory master clock is chosen according to its long term stability behaviour as deduced by the IEN intercomparisons and from the bi-monthly rates versus the international atomic time scale data published by the BIPM[7]. The master clock frequency is supplied to a phase microstepper whose rate is periodically adjusted to maintain UTC(IEN) in agreement within 5 us with UTC established by the BIPM.

Since mid-1985, the IEN time scale is compared with UTC by means of the Global Positioning System satellites, according to the common view measurement schedule. This change in the international synchronization link used by IEN as well as by many other laboratories has significantly improved the accuracy of the time comparisons [8] allowing new investigations on periodic rate changes in atomic clocks.

In Fig. 1, the equipment set up for the IEN time scale realization is depicted, meanwhile, in Fig. 2, its behaviour against UTC time scale in the last three years is shown.

Table 1 reports the IEN master clock rate corrections performed by means of the phase microstepper to maintain UTC(IEN) in close agreement with UTC in the period 1985-1987.

Table 1

MJD	Date	Master Clock	UTC(IEN) - Master Clock (ns/d)
46213	1985 May 28	Cs5061A-004 sn893	+34
46473	1986 Feb 12	"	+10
46723	1986 Oct 20	"	+32
46913	1987 Apr 28	"	+16
46983	1987 Jul 8	"	+28

Looking carefully at the shape of the UTC(IEN) graph it can be seen that a seasonal effect is present and that the rate compensation performed on the phase microstepper has not eliminated this effect.

Moreover the time scale generated directly by the master clock, as reported in

Fig. 3, would have been more uniform without the use of the microstepper, but with a total time error exceeding our stated limits. This consideration showed the importance of a careful characterization of the long term behaviour of every IEN clock to find out if seasonal effects were detectable in order to optimize the time scale corrections.

The environmental conditions of the clock room, as regards temperature and absolute humidity, measured in the period 1985-1987 are reported in Fig. 4. It can be noticed that, while the temperature is stable within $\pm 0.5^\circ\text{C}$, the absolute humidity can vary from about 8 gm^{-3} to 18 gm^{-3} (about 40% to 80% relative humidity) (*).

This is due to the fact that in this room only the temperature is controlled by means of a heater switched on automatically by a temperature sensor meanwhile no humidity control is made and therefore the external variation is followed with nearly a 10 days delay.

A first attempt in analyzing the long term behaviour against UTC of some cesium clocks at IEN in Torino and at the Istituto Superiore Poste e Telecomunicazioni (ISPT) in Roma [9] showed the presence of seasonal effects. However it turned out necessary to improve the investigation tools by adopting suitable mathematical models and statistical treatments.

3. Measurements set-up and synchronization links used

The time differences between UTC(IEN) and the IEN cesium clocks analyzed and reported in this paper are ten day averages of the values measured daily at 00h UTC with a 1 ns resolution.

Concerning the ISPT cesium clocks, the measurement resolution is the same, but they are referred to UTC(IEN) by means of daily television measurements having a typical standard deviation of 50 ns (1σ). This laboratory has both humidity and temperature controls.

As the IEN has only commercial cesium standards, all the clocks readings have been referred to UTC, by means of the corrections of UTC(IEN) published by BIPM, assuming that the international atomic time scale is less sensitive to seasonal effects being made up by a large number of clocks kept in different locations and environments.

The IEN and ISPT temperature and absolute humidity data, have also been averaged

(*) In practice, in the clocks room the relative humidity in % is measured. These values have been converted into absolute humidity data, expressed in gm^{-3} , using the conversion coefficients given by the Smithsonian Physical tables, related to the room temperature.

over ten days from the daily readings taken by the data acquisition systems with resolution of .1 K and of 5%.

4. Mathematical models for seasonal variations

When dealing with seasonal variations it is helpful to use a simple but adequate mathematical model to extract quasi-periodic variations from drifts and statistical fluctuations. In this paper two different attempts have been performed.

With the first approach we approximate the long term behaviour of the time difference between a time reference and a cesium clock with the function

$$f(x) = a + bx + \frac{1}{2}cx^2 - d \cos \omega x \quad (1)$$

where: x is expressed in days, $f(x)$ in microseconds, ω , the angular frequency, is equal to $2\pi/(365 \text{ days})$. The variable x ranges from 0 to $k \cdot 365$ while ωx varies from 0 to $k \cdot 2\pi$, where k is an integer number. The parameters a, b, c, d can be calculated by subsequent numerical derivations, assuming that the period of the sinusoidal part is exactly 365 days and analyzing the data relative to an integer number of periods to be sure that the mean value of $\cos \omega x$ is null.

This method gives satisfactory results but the differentiation magnifies the irregularities of the data and therefore it is necessary a smoothing process at each derivation step. On the contrary, a method based on an integration process does not present this kind of problem.

Considering always an integer number of periods, we can calculate the first terms of a Fourier series, obtaining:

$$\begin{aligned} \int_0^{2\pi} f(x) d\omega x &= 2\pi a + \frac{4\pi^3 c}{3\omega^2} \\ \int_0^{2\pi} f(x) \sin \omega x d\omega x &= -\frac{2\pi b}{\omega} \\ \int_0^{2\pi} f(x) \cos \omega x d\omega x &= -d\pi + \frac{2\pi c}{\omega^2} \\ \int_0^{2\pi} f(x) \cos 2\omega x d\omega x &= \frac{\pi c}{2\omega^2} \end{aligned} \quad (2)$$

Operating by numerical integration and substitution in Equations (2), the values of the coefficients a, b, c, d are obtained.

It turns out that these two methods give almost the same results.

The experimental data can also be fitted to an arbitrary function, for example

with the Gauss-Newton method [10] which satisfies the least-squares approximation. This iterative process has been applied to the experimental data and stopped when the relative parameter variations were lower than 10^{-4} . It has been estimated more suitable to use in the calculations the normalized frequency departures data of each clock considered. Therefore the fitting curve defined in (1) is modified into

$$h(x) = \frac{f_{cs} - f_{ref}}{f_{ref}} = - (dw \sin wx + b + cx) / .00864 \quad (3)$$

where the numerical factor allows to express $h(x)$ in 10^{-13} . The parameters values so obtained are the best approximation as far as the least-squares regression is concerned. Moreover the possible initial phase shift has been introduced and evaluated to avoid any subjective estimate of the time origin of the sine function. Consequently the final fitting function is

$$h(x) = - [dw \sin w(x + e) + b + cx] / .00864 \quad (4)$$

where e is expressed in days.

As a last step, the statistical fluctuations can be computed as the residual between the experimental data and the approximating curve $h(x)$. These fluctuations can be analyzed by means of the Allan variance to characterize the kind of frequency noises affecting the clocks. An example of this statistical computation, performed on Cs9, is given in Table 2. A white frequency noise can be evinced from this data.

Table 2

τ [d]	$\sigma_y(\tau) [10^{-14}]$
10	5.8
20	6.1
40	4.8
80	3.1
160	2.4

The amount of the seasonal fluctuations has been determined as well through a

second approach based only on statistical treatments. A cesium standard phase variation with respect to a reference is assumed to be of the form

$$\Phi = \omega_0 t + \varphi_0 + \sum_{k=2}^N \frac{\Omega_{k'}}{k!} t^k + \sum_m a_m(t) \sin[\omega_m t + \theta_m(t) + \theta_{0m}] + \varphi(t) \quad (5)$$

where ω_0 and ω_m are angular frequencies of operation and of periodic seasonal effects respectively, $\Omega_{k'}/k!$ are long term phase drift coefficients, $a_m(t)$, $\theta_m(t)$ and $\varphi(t)$ are random variables. Seasonal variations can be evaluated by computing variances if the polynomial drift is unimportant either because it is very small, in the sample time of interest, compared with periodic modulations, or it is removed by using Hadamard variances on sets of a suitable number M of adjacent samples weighted with binomial coefficients [11,12].

In the following, the expressions concerning the simple special cases of the two-sample variance σ_Y^2 and of the Hadamard variance $\langle \sigma_{HBC}^2(M, \tau, \tau) \rangle$ with $M = 3$ are reported.

For sake of simplicity $\sum_m a_m(t)$ is substituted with $a(t)$ whose mean value and variance are μ_a and σ_a^2 respectively, moreover the correlation coefficients of the fluctuations of $a(t)$ and $\theta(t)$ are supposed to be zero for the time intervals of the order and/or longer than half a year. The same hypothesis is assumed for all the other covariance coefficients.

For the Allan variance case, if contributions from all $\Omega_{k'}$ are negligible, the following expressions are obtained:

$$\sigma_Y^2 = \sigma_{Y,\varphi}^2 + \left(\frac{\mu_a}{\omega_0 \tau}\right)^2 \left\{ \sin^2 \theta_0 \left[\frac{3}{2} \left(1 + \frac{\sigma_a^2}{\mu_a^2}\right) (1 + e^{-2\sigma_\theta^2}) + 5e^{-\sigma_\theta^2} \right] + \right. \\ \left. + \cos^2 \theta_0 \left[\frac{3}{2} \left(1 + \frac{\sigma_a^2}{\mu_a^2}\right) (1 - e^{-2\sigma_\theta^2}) \right] \right\} \quad (6a)$$

if $\omega_m \tau = \pi$, and

$$\sigma_Y^2 = \sigma_{Y,\varphi}^2 + \left(\frac{\mu_a}{\omega_0 \tau}\right)^2 \left\{ \frac{3}{2} \left(1 + \frac{\sigma_a^2}{\mu_a^2}\right) + e^{-\sigma_\theta^2} (-2 \cos \omega_m \tau + \frac{1}{2} \cos 2 \omega_m \tau) \right\} \quad (6b)$$

if $\omega_m \tau \neq \pi$.

In (6a) and (6b) σ_θ^2 is the variance of $\theta(t)$ and $\sigma_{Y,\varphi}^2$ is the Allan variance of the process $\varphi(t)$.

For the Hadamard variance ($M = 3$), under the same assumptions stated before, the following expressions hold:

$$\langle \sigma_{H_{BC}}^2(3, \tau, \tau) \rangle = \sigma_{H_{BC}, \varphi}^2 + \left(\frac{\mu_a}{\omega_0 \tau} \right)^2 \left\{ \sin^2 \vartheta_0 \left[10 \left(1 + \frac{\sigma_a^2}{\mu_a^2} \right) \left(1 + e^{-2\sigma_0^2} \right) + 44 e^{-\sigma_0^2} \right] + \right. \\ \left. + \cos^2 \vartheta_0 \left[10 \left(1 + \frac{\sigma_a^2}{\mu_a^2} \right) \left(1 - e^{-2\sigma_0^2} \right) \right] \right\} \quad (7a)$$

if $\omega_m \tau = \pi$, and

$$\langle \sigma_{H_{BC}}^2(3, \tau, \tau) \rangle = \sigma_{H_{BC}, \varphi}^2 + \left(\frac{\mu_a}{\omega_0 \tau} \right)^2 \left\{ 10 \left(1 + \frac{\sigma_a^2}{\mu_a^2} \right) + \right. \\ \left. + e^{-\sigma_0^2} \left(-15 \cos \omega_m \tau + 6 \cos 2\omega_m \tau - \cos 3\omega_m \tau \right) \right\} \quad (7b)$$

if $\omega_m \tau \neq \pi$.

Useful simpler expressions can be obtained to evaluate the effects of small fluctuations in $a(t)$ and $\vartheta(t)$, that is when $\sigma_0^2 \ll 1$ and $\sigma_a^2 / \mu_a^2 \ll 1$. If these fluctuations are entirely negligible, the substitutions $\sigma_a^2 = \sigma_0^2 = 0$ in (6) and (7) lead to the following results for periodic contributions:

$$\sigma_Y^2 = 8 \left(\frac{\mu_a}{\omega_0 \tau} \right)^2 \sin^2 \vartheta_0 \quad \text{if } \omega_m \tau = \pi \quad (8a)$$

$$\sigma_Y^2 = 4 \left(\frac{\mu_a}{\omega_0 \tau} \right)^2 \sin^4 \frac{\omega_m \tau}{2} \quad \text{if } \omega_m \tau \neq \pi \quad (8b)$$

$$\langle \sigma_{H_{BC}}^2(3, \tau, \tau) \rangle = 64 \left(\frac{\mu_a}{\omega_0 \tau} \right)^2 \sin^2 \vartheta_0 \quad \text{if } \omega_m \tau = \pi \quad (9a)$$

$$\langle \sigma_{H_{BC}}^2(3, \tau, \tau) \rangle = 32 \left(\frac{\mu_a}{\omega_0 \tau} \right)^2 \sin^6 \frac{\omega_m \tau}{2} \quad \text{if } \omega_m \tau \neq \pi \quad (9b)$$

In the special case $\omega_m \tau = \pi$ the two variances exhibit the same dependence on ϑ_0 , whereas for $\omega_m \tau \neq \pi$ these simpler expressions show that the Hadamard variance is more selective. The curves of $\sigma_Y^2 / [4(\mu_a / \omega_0 \tau)^2]$ and of $\langle \sigma_{H_{BC}}^2(3, \tau, \tau) \rangle / [32(\mu_a / \omega_0 \tau)^2]$ referring to a sinusoidal deterministic process are compared in Fig. 5.

5. Evaluations of the seasonal variations

The mathematical and statistical processes mentioned in Section 4 have been applied to the cesium clocks kept at IEN and at ISPT. In Table 3 the model, the serial number and the period of observation, in Modified Julian Date (MJD), are reported for each clock.

Table 3

Laboratory	Clock Manufacturer and model	Serial number	Abbreviation used	Observation period	
				(days)	from-to (MJD)
ISPT	HP5061A/004	597	Cs1	450	46229-46679
	HP5061A/004	1815	Cs3	570	46489-47059
IEN	HP5061A	609	Cs5	660	46229-46889
	HP5061A/004	893	Cs6	730	46229-46959
	OSA3200	84	Cs9	830	46229-47059

The normalized frequency departure versus UTC with a constant value subtracted and the frequency drift removed are reported for each clock in Fig. 6 and Fig. 7. The results obtained by fitting the experimental data using the Gauss-Newton method have been plotted over the same graphs, while the associated parameters are summarized in Table 4.

Table 4

Clock	Parameters			
	b [10^{-13}]	c [10^{-13} /yr]	ω d [10^{-13}]	e [d]
Cs1	-1.0	-2.5	-0.6	30
Cs3	-2.9	0.9	-0.5	-30
Cs5	8.0	-0.2	1.2	0
Cs6	2.5	-0.4	1.1	0
Cs9	15.2	0.6	-2.4	40

The coefficients b, c, d, e are those found in equation (4) and represent respectively:

- b: the mean frequency departure at $x = 0$,
- c: the frequency drift,
- ωd : the amplitude of the sinusoidal term,
- e: the initial phase (divided by ω) at $x = 0$.

In the lower side of Fig. 6 and Fig. 7, the temperature and the absolute humidity variations for both IEN and ISPT laboratories have also been reported.

The analysis through the Allan and the Hadamard variances was performed only on the Cs6 and Cs9 IEN standards for the last two years. The statistical data reported here below are extracted from reference [13].

The Hadamard variance was used to remove possible linear frequency drifts, but the results obtained did not give any more information on periodic oscillations and on medium term instabilities. As a consequence from the data of both the Allan and Hadamard variances it was suggested that frequency drifts were negligible in Cs6 and Cs9 in the sample time considered and this conclusion was confirmed through the Gauss-Newton method too.

Cs9 Allan variance diagrams referring to two different starting times for computations are shown in Fig. 8 where seasonal variations appear in the range 25-250 days. The time difference between the start points in the two graphs is 90 days which corresponds to $\Delta\theta_0$ close to $\pi/2$ and they were chosen so that θ_0 values are close to 0 and $\pi/2$. Note that in this figure the horizontal axis reports days, one day being approximately 1 degree. The minimum and maximum values occur for sampling times equal to 170 days. Some irregularities may be ascribed to the small number of data available for the averages. In effect the θ_0 dependence of σ_y^2 , as obtained from many graphs, is shown in Fig. 9 and Fig. 10 for Cs9 and Cs6 respectively. It is strong and nearly equal for $\tau = 170$ and 180 days whereas it decreases for $\tau = 160$ days.

A rough estimate of seasonal variations is obtained by using the very simple expressions (8a) and (8b) which strictly refer to a deterministic periodic process. The factor $(\mu_a/\omega_0\tau)^2 = (\mu_a\omega_m/\omega_0)^2\tau^2$ in the non-stationary case $\omega_m\tau = \pi$ can be easily evaluated. In fact $\mu_a\omega_m/\omega_0$ turned out to be 2.5×10^{-13} and 1.1×10^{-13} for Cs9 and Cs6 respectively. These results are in agreement with those reported in Table 4, noting that $\mu_a\omega_m/\omega_0 = \omega d$ of expression (4).

Some conclusions can be argued about the cloks analyzed. Looking at Fig. 7, where the mean frequency departures of Cs1 and Cs3 of ISPT together with temperature and humidity diagrams are reported, and analyzing the coefficients of Table 4, it is suggested that the amounts of their frequency variations (ωd of the order of 1×10^{-13} peak to peak) cannot be easily related to the humidity variations only, these last being rather small whereas the temperature varying about 0.5°C.

On the other hand the ISPT clocks synchronization link used to relate them to UTC is considerable noisier than that used for IEN clocks and therefore the interpolation results have a low confidence level. As far as the IEN cesium clocks are concerned (Fig. 6), the amounts of seasonal fluctuations range from 2 to 5 times 10^{-13} . If temperature variation effects are supposed to be negligible compared to those of humidity, we can ascribe to these latter the observed frequency variations. Under this hypothesis the coefficients of fractional frequency variations per absolute humidity variations ($10^{-15}/\text{g m}^{-3}$) are evaluated to be 24 for Cs5, 22 for Cs6 and -48 for Cs 9. These results are in agreement with the evaluations reported in [2]. Moreover a delay between frequency and humidity variations, ranging from some days to one month and depending on the type of clock, has been pointed out. According to this observation it seems possible to find out a suitable time, for each clock, in order to compensate the seasonal effect and to improve the uniformity of the IEN time scale.

6. Conclusions

In this work, the presence of seasonal effects on five commercial cesium clocks has been detected and the relative amount has been evaluated.

Two different approaches of evaluation have been experimented obtaining consistent results and a good agreement has been also found with previous investigations. At this point, it appears possible to elaborate suitable criteria of a time scale seasonal effect compensation and to maintain UTC(IEN) within 2 microseconds.

References

- [1] S. Iijima, K. Fujiwara, H. Kobayashi, T. Kato: Effect of environmental conditions on the rate of a cesium clock - Annals of the Tokio Astronomical Observatory, Second Series, vol. XVIII, n. 1, p. 50-67.
- [2] G. Becker: Zeitskalenprobleme: jahreszeitliche Gangschwankungen von Atomuhren, PTB Mitteilungen 92 2/82, p. 105-113.
- [3] K. Dorenwendt: Das Verhalten kommerzielle Cäsium-Atomuhren und die Zeitskalen der PTB - PTB Mitteilungen 94, p. 35-43.
- [4] A. De Marchi: Understanding environmental sensitivity and ageing of cesium beam frequency standards - Proceedings 1st European Frequency and Time Forum, Besançon (France), March 1987.
- [5] J. Kusters: New 5061A Specifications: Temperature Performance - Hewlett-Packard - The Standard, October 1983.
- [6] F. Cordara, V. Pettiti: Time keeping and time and frequency dissemination at the Istituto Elettrotecnico Nazionale (IEN) - 18th Precise Time and Time Interval Meeting, Washington D.C., Dec. 1986.
- [7] BIH Annual Reports and Circulars D.
- [8] J. Azoubib, B. Guinot: Use of GPS time comparisons for establishing TAI in 1983 and related problems - Bureau International de l'Heure - Notes internes, n. 1, June 1984.
- [9] F. Cordara, V. Pettiti, G. Tignanelli: Environmental effects on cesium clocks kept at IEN - Torino and ISPT - Roma Time and Frequency laboratories - Proceedings 1st European Frequency and Time Forum, Besançon (France), March 1987.
- [10] N.R. Draper, H. Smith: Applied Regression Analysis - 2nd ed. Wiley, New York, 1981.
- [11] W.C. Lindsey, C.M. Chie: Theory of Oscillator Instability Based Upon Structure Functions - Proc. IEEE, vol. 64, Dec. 1976, p. 1652-1666.
- [12] J. Rutman: Characterization of Phase and Frequency Instabilities in Precision Frequency Sources: Fifteen years of Progress - Proc. IEEE, vol. 66, Sep. 1978, p. 1048-1075.
- [13] P. Briatore, M. Fasolis: Caratterizzazione statistica dell'instabilità di frequenza di oscillatori campione - Tesi di Laurea in Ingegneria Elettronica, Politecnico di Torino, Dec. 1987.

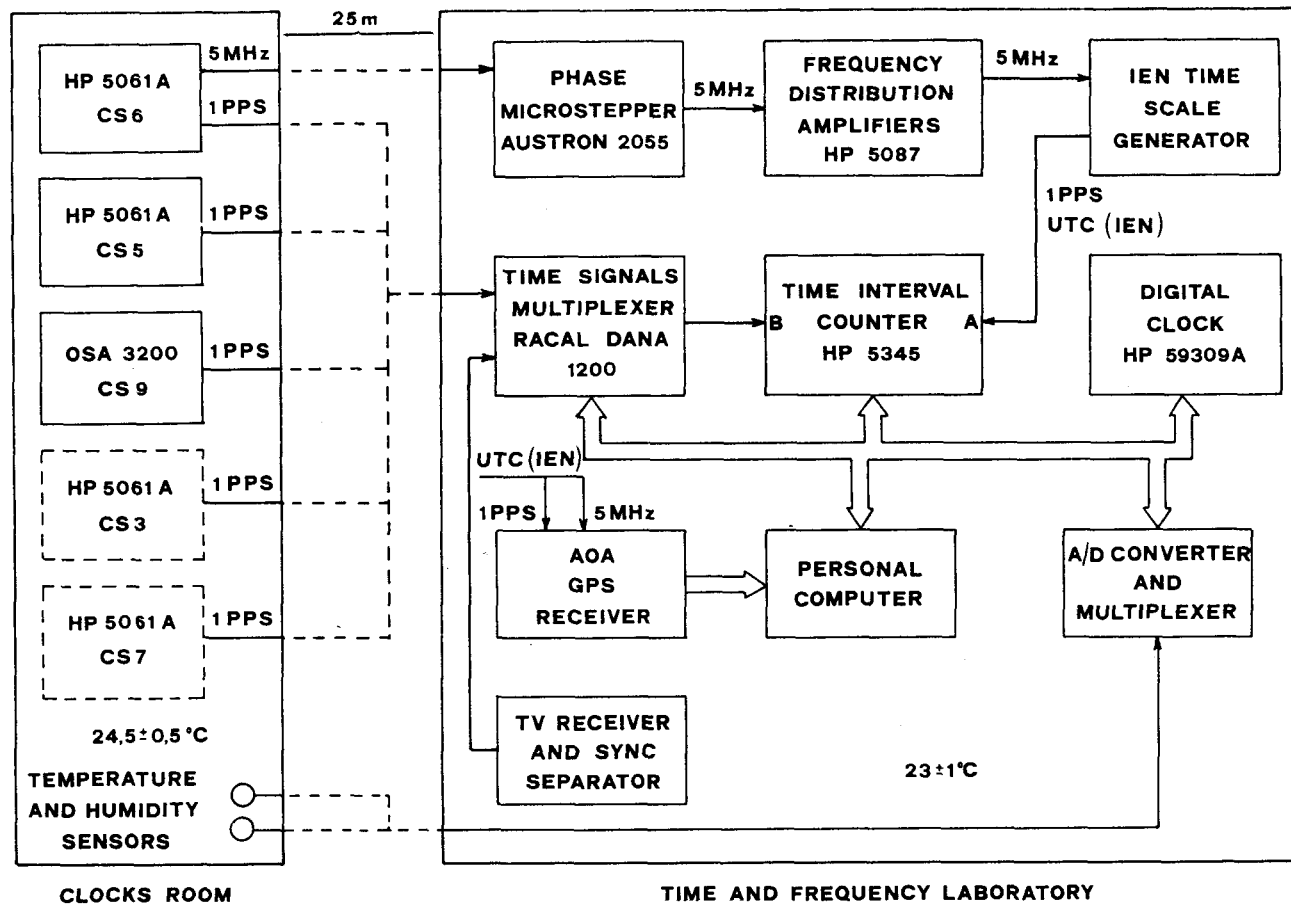


Fig. 1 - Equipment used to realize UTC(IEN) and to perform clocks intercomparisons.

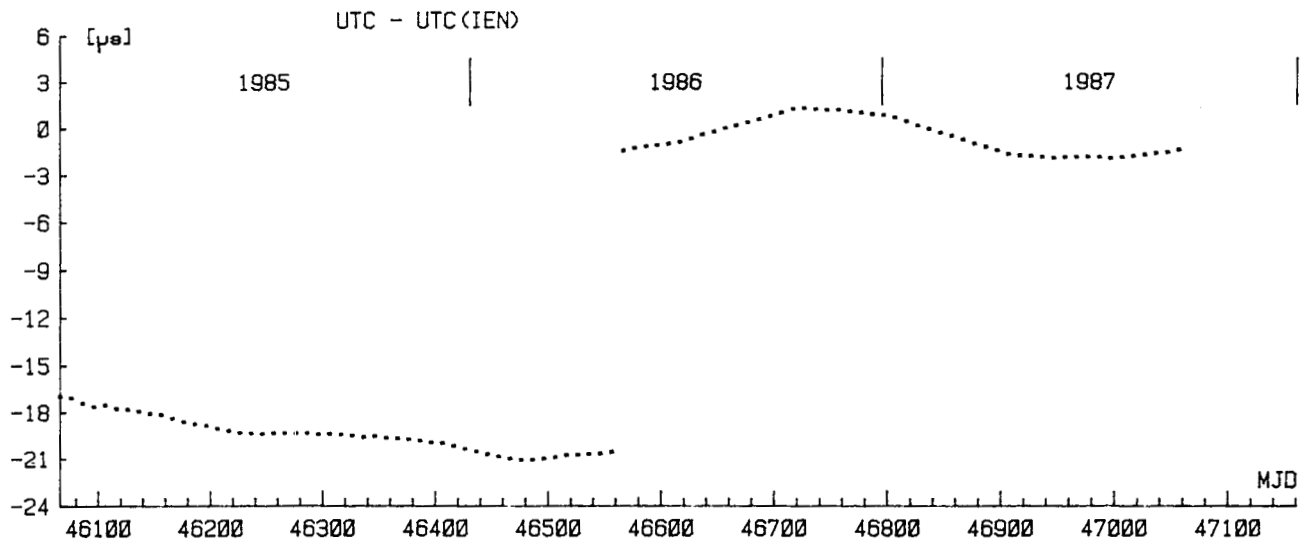


Fig. 2 - UTC(IEN) vs. UTC from BIPM/BIH Annual Report and circulars D.

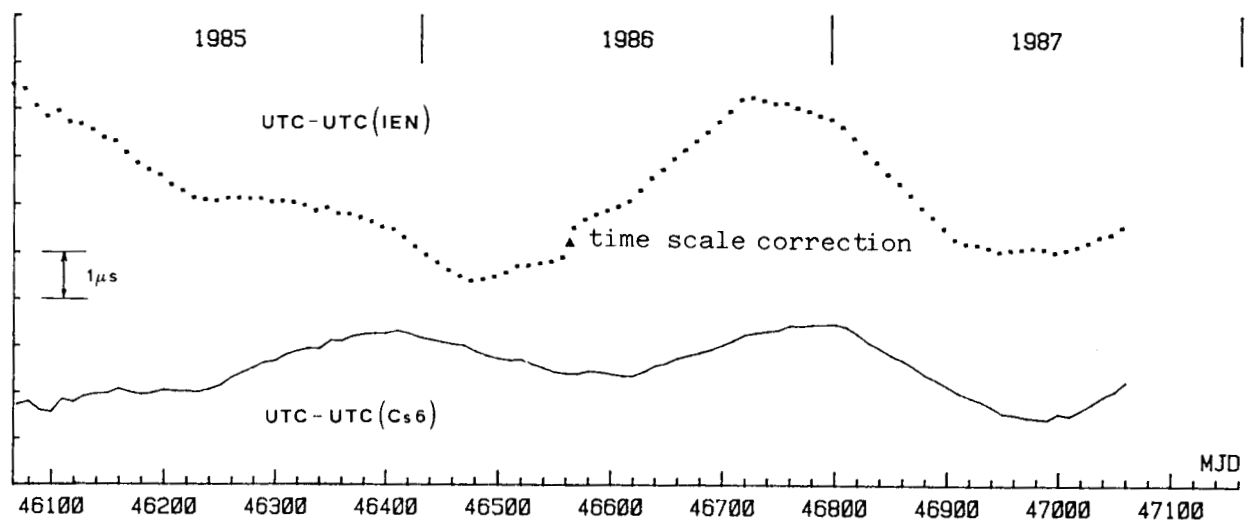


Fig. 3 - UTC(IEN) vs. UTC compared with UTC(Cs6) vs. UTC. The mean rate of Cs6 is subtracted.

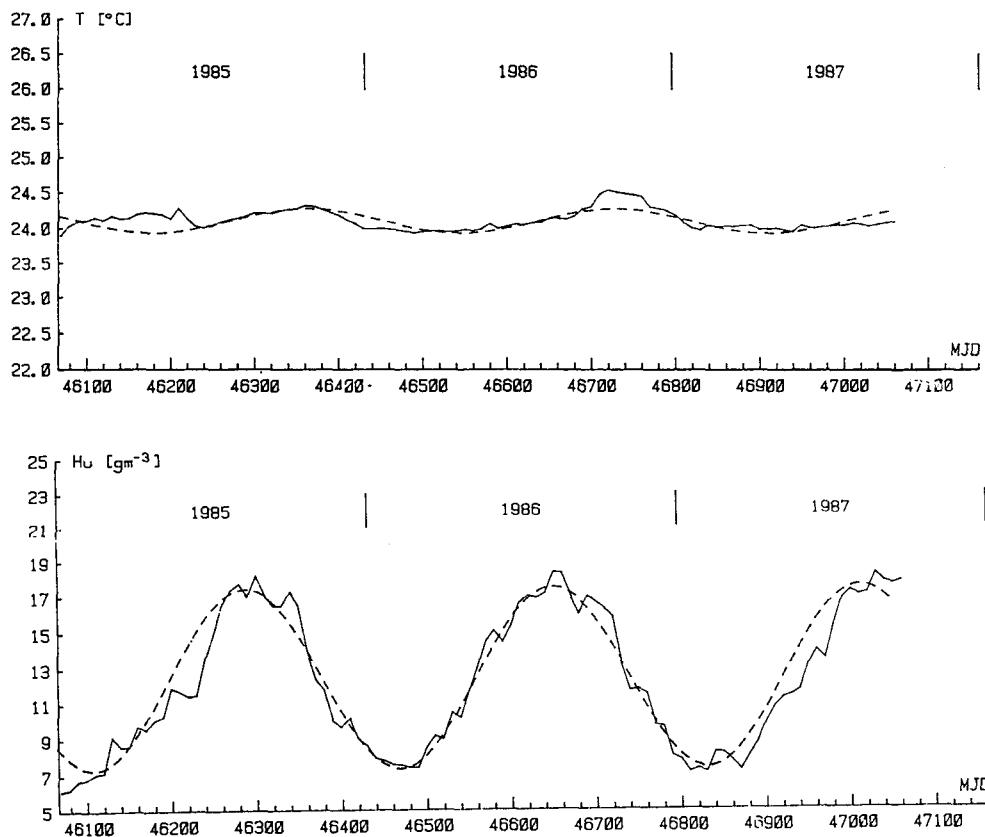


Fig. 4 - IEN clock room temperature (T) and absolute humidity (Hu) diagrams.

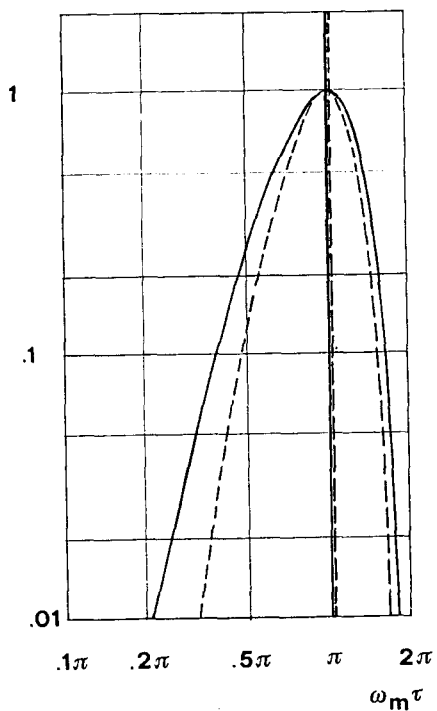


Fig. 5 - Normalized Allan and Hadamard variances for periodic modulation

$$\text{---} \sigma_y^2 / 4(\mu_a / \omega_0 \tau)^2$$

$$\text{---} \langle \sigma_{HBC}^2(3, \tau, \tau) \rangle / 32(\mu_a / \omega_0 \tau)^2$$

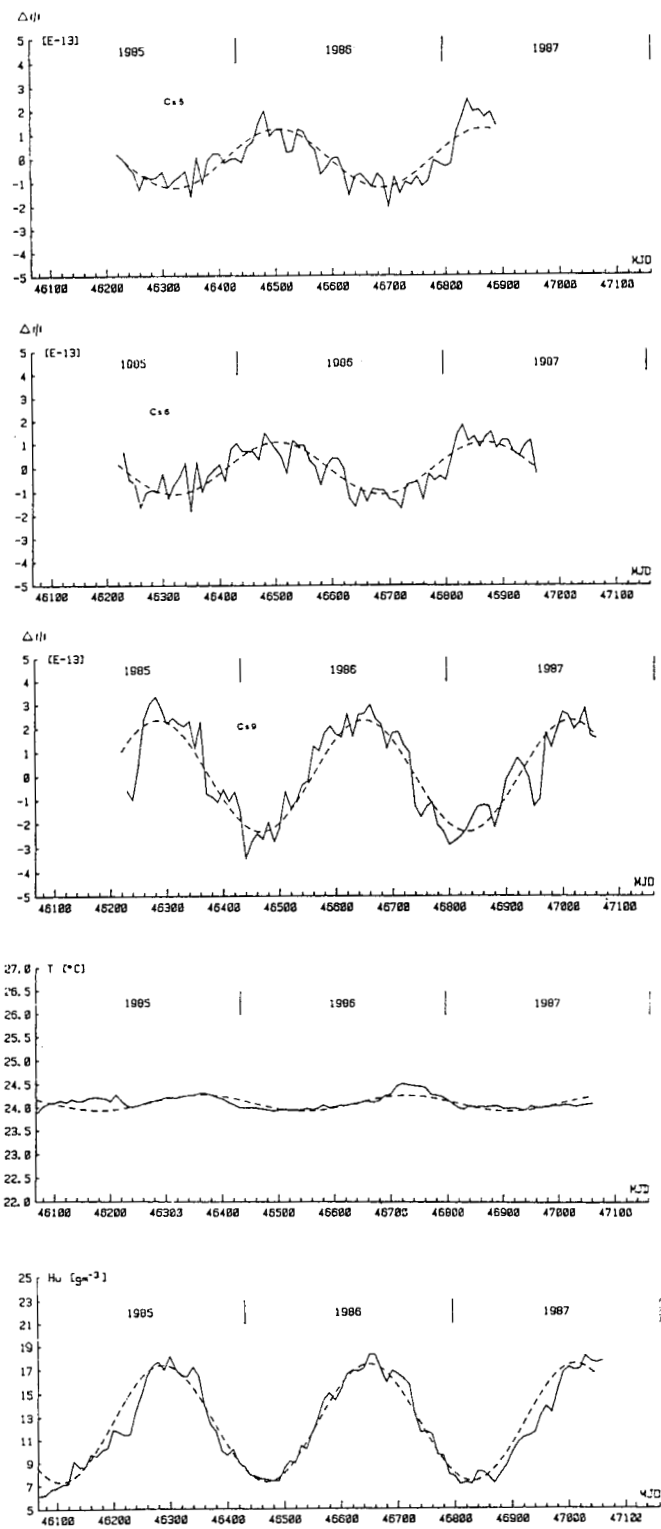


Fig. 6 - Normalized frequency departures of IEN cesium clocks vs. UTC, temperature (T) and absolute humidity (Hu) of the clocks room.

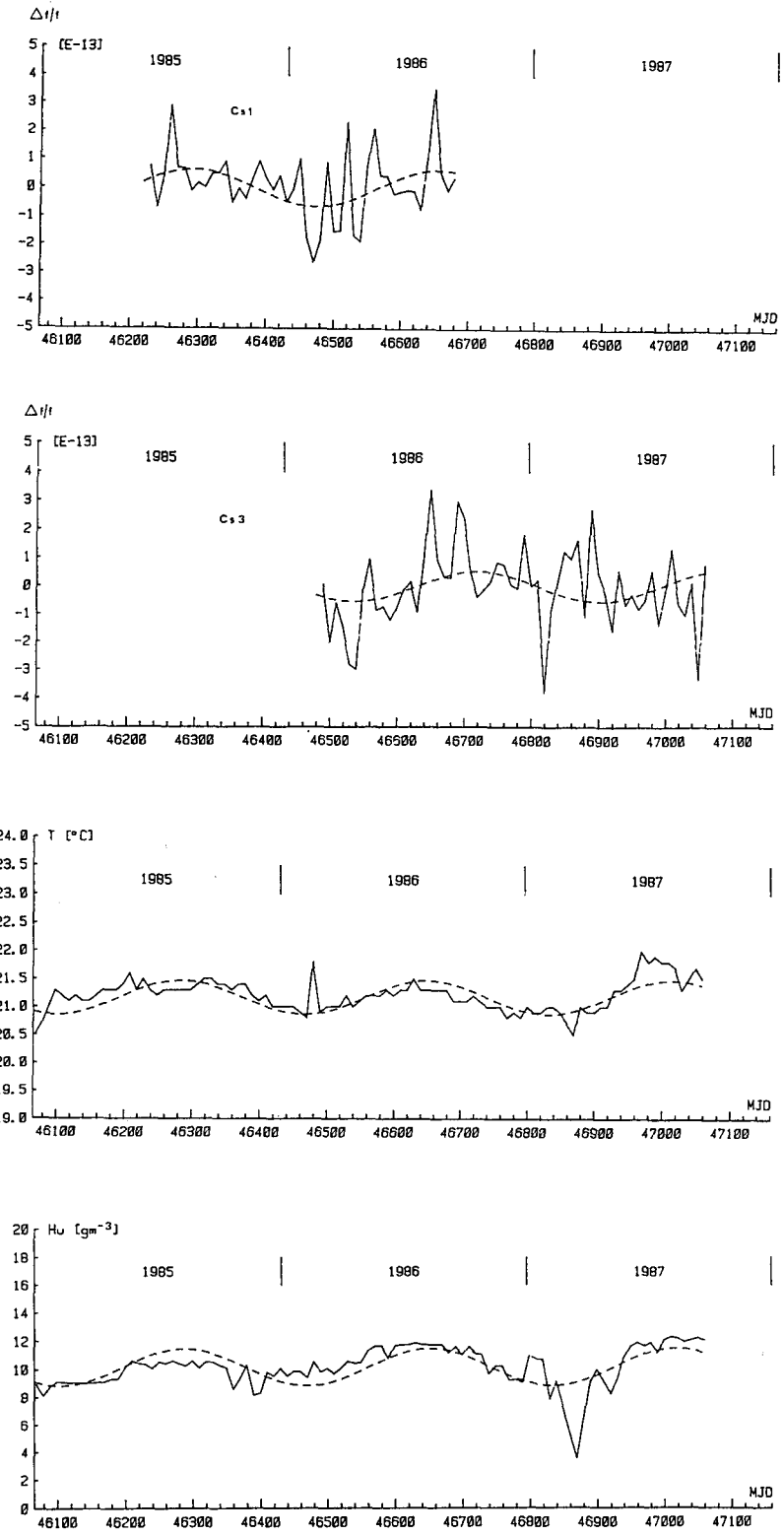


Fig. 7 - Normalized frequency departures of ISPT cesium clocks vs. UTC, temperature (T) and absolute humidity (Hu) of the clocks room.

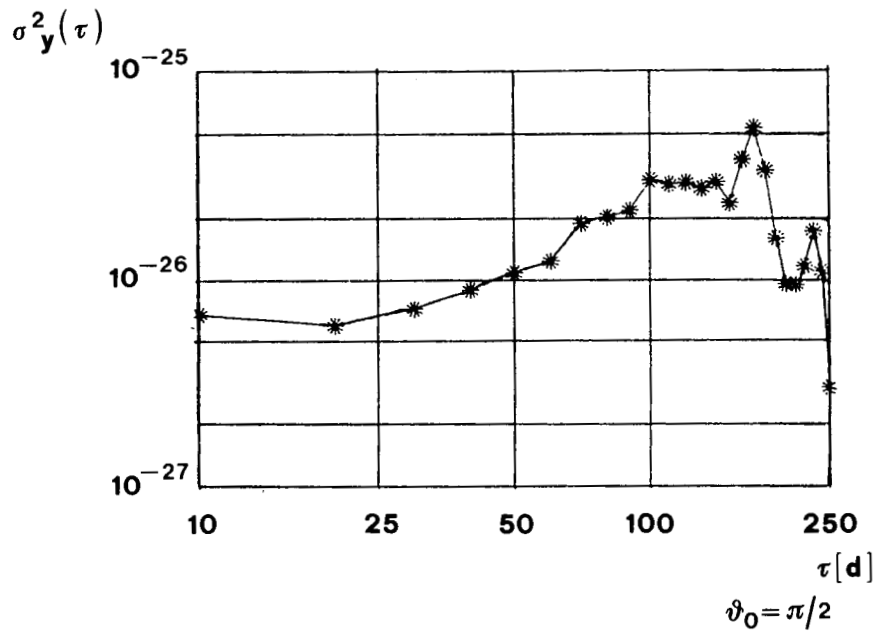
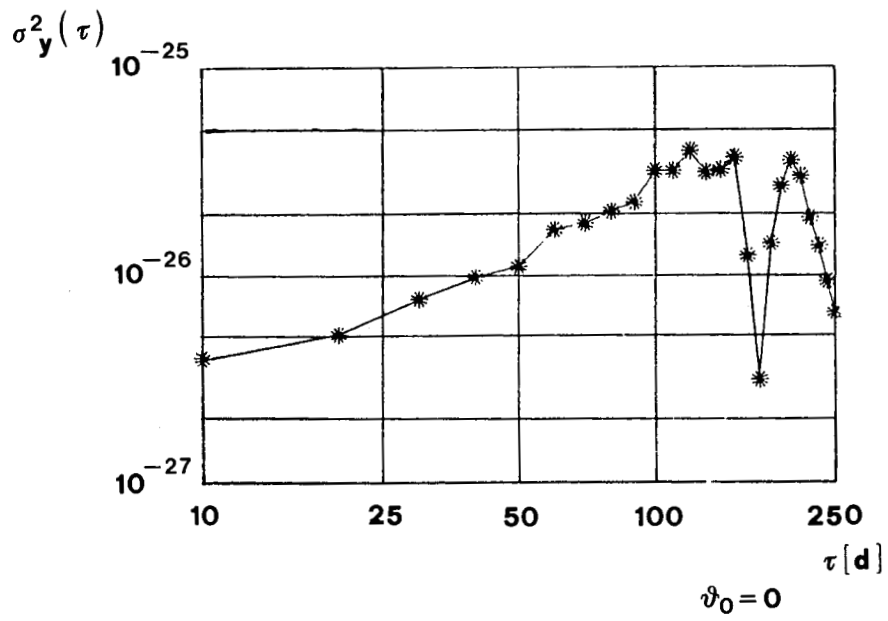


Fig. 8 - Allan variance computed for the Cs9 with two different starting times.

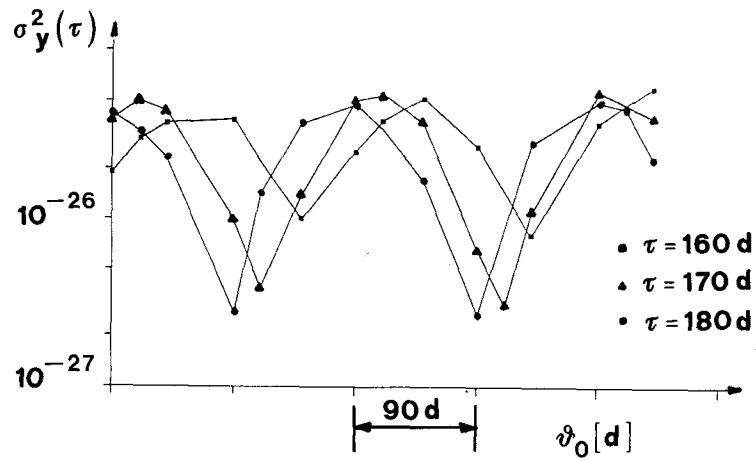


Fig. 9 - $\sigma_y^2(\tau)$ of Cs9 vs. the measurement starting point or phase θ_0 for three τ values.

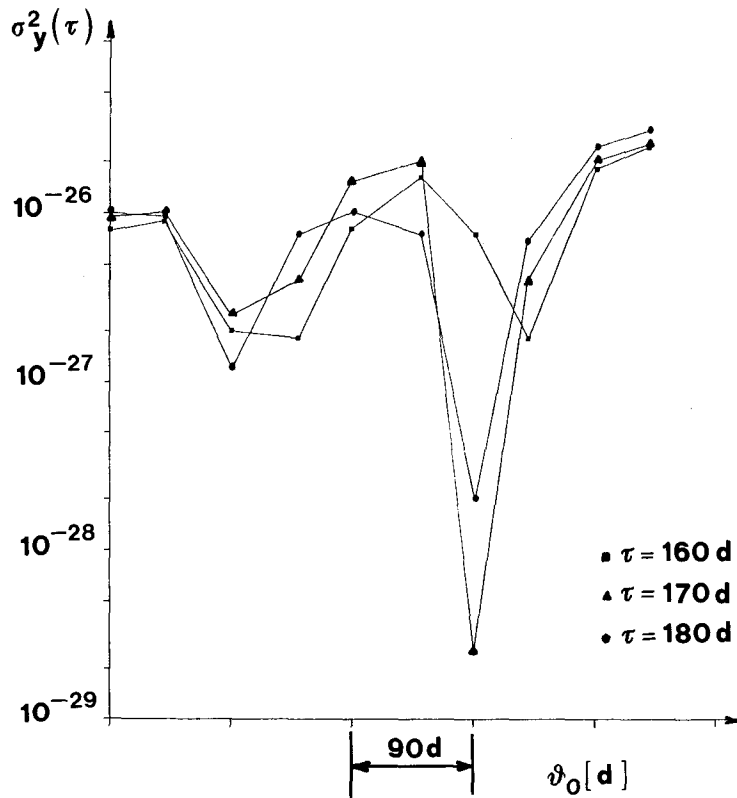


Fig. 10 - $\sigma_y^2(\tau)$ of Cs6 vs. the measurement starting point or phase θ_0 for three τ values.